ACCSCIENCE PUBLISHING

Asian Journal of Water, Environment and Pollution

ORIGINAL RESEARCH ARTICLE

Spatiotemporal dynamics and stability of wave energy resources for southern Vietnamese islands: A climate-scale assessment (1995–2025)

Tran Thi Mai Huong[1,2,3], Le Thanh Phong[2,3], Nguyen Xuan Kha[2,3], Nguyen Tuan[1,3], and Dang Truong An[1,3]*

[1]Faculty of Physics and Engineering Physics, University of Science, Ho Chi Minh City, Vietnam

[2]Faculty of Geology and Petroleum Engineering, University of Technology, Ho Chi Minh City, Vietnam

[3]Vietnam National University, Ho Chi Minh City, Vietnam

Abstract

Offshore island and nearshore energy systems in southern Vietnam remain constrained by diesel dependence, fuel-logistics risks, and carbon emissions. This study applies a Delft3D-WAVE/SWAN framework forced by hourly ERA5 winds to quantify significant wave height (Hs), peak period (Tp), and finite-depth wave-power density at six strategic locations over 1995–2025. Model skill was evaluated against *in situ* acoustic wave and current observations. Hs performance was strong at Ca Mau ($R = 0.90$; Willmott $d = 0.93$) and moderate at Ben Tre ($R = 0.70$; $d = 0.60$), whereas Tp skill was weaker, especially at Ben Tre; wave-period-dependent results are therefore interpreted cautiously. A sharp east–west resource gradient was identified: Phu Quy had the highest mean power (13.87 kW/m) and P_{95} (60.10 kW/m), followed by Con Dao and Tra Vinh. Significant positive wave-power trends occurred at Phu Quy (+0.1436 kW/m/yr; $p = 0.005$), Tra Vinh (+0.0795 kW/m/yr; $p < 0.001$), and Vung Tau (+0.0563 kW/m/yr; $p < 0.001$). The dominant directional sector contributed 56.4–73.5% of annual energy at the eastern stations and exceeded 70% at Phu Quy and Con Dao. An equal-weight, min–max-normalized Long-term Suitability Score ranked Phu Quy and Tra Vinh first and second; both positions were stable when each criterion weight was varied by ±20%. The findings provide a multi-decadal resource-screening basis for marine spatial planning, while the device yield, future-climate response, and hybrid-system performance require dedicated techno-economic and scenario analyses.

Keywords: Wave energy resources; Monsoon seasonality; Southern Vietnamese islands; Long-term trends; Offshore energy systems

***Corresponding author:**
Dang Truong An
(dtan@hcmus.edu.vn)

Citation: Huong TTM, Phong LT, Kha NX, Tuan N, An DT. Spatiotemporal dynamics and stability of wave energy resources for southern Vietnamese islands: A climate-scale assessment (1995–2025). *Asian J Water Environ Pollut.* 2026;23(5):026280191. doi: 10.36922/AJWEP026280191

Received: July 15, 2026

Revised: August 25, 2026

Accepted: August 31, 2026

Published online: September 30, 2026

Copyright: © 2026 Author(s). This is an Open-Access article distributed under the terms of the Creative Commons Attribution License, permitting distribution, and reproduction in any medium, provided the original work is properly cited.

Publisher's Note: AccScience Publishing remains neutral with regard to jurisdictional claims in published maps and institutional affiliations.

1. Introduction

The global imperative to transition toward low-carbon energy systems has intensified in recent years, driven by the acute challenges of climate change and the collective commitment to the "Net Zero 2050" targets established under the Paris Agreement.[1-3] Within this framework, marine renewable energy (MRE) has emerged as a cornerstone for national energy security strategies, particularly for coastal and maritime nations. Among ocean-based resources, wave energy has one of the highest energy densities and

shows greater temporal persistence than solar and wind power.[4-6] A critical advantage of wave energy is its ability to complement purely atmospheric renewables; ocean waves integrate wind forcing over vast fetches, acting as a natural energy storage mechanism that provides a smoother, more predictable resource profile.[4,6,7] By integrating wave power into the energy mix, the inherent intermittency of solar and wind generation can be substantially mitigated, thereby enhancing the overall reliability of isolated microgrids.[8,9]

For remote island communities and nearshore economic zones, the energy problem is not merely a question of resource abundance but of logistical survival. Many island systems remain constrained by heavy dependence on diesel-fueled power generation, which exposes local communities to fuel-price volatility, shipping disruptions, and high carbon emissions.[1,2] Consequently, there is an urgent technological need for wave-energy converter (WEC) systems that are specifically adapted to island environments. Recent advancements in WEC technology, such as point absorbers,[6,7] oscillating water columns,[10,11] and oscillating surge converters,[6,7] offer scalable solutions for decentralized power supply. Furthermore, integrating these devices into existing coastal infrastructure, such as harbor breakwaters or multi-use marine platforms, can significantly reduce installation costs and environmental footprints, making small-to-medium-scale wave-energy applications operationally feasible for island-scale microgrids.[8,9]

Vietnam, with its extensive coastline and vast maritime territory comprising over 3,000 islands, holds immense potential for marine renewable energy development. However, the wave climate across the Vietnamese shelf is characterized by complex hydrodynamic interactions and strong spatial gradients.[12] While previous assessments have focused on the central coast because of its high-energy sea states, the southwestern shelf, stretching from Vung Tau to Kien Giang, remains insufficiently quantified. This region sits on a broad, shallow continental shelf where coastal morphology and numerous islands, such as the Con Dao archipelago, Phu Quy, and Phu Quoc, create significant sheltering effects.[12,13] The regional wave climate is fundamentally governed by the seasonal reversal of the Asian monsoon system, where the northeast monsoon generates dominant swells from the East Sea, while the southwest monsoon produces weaker, more variable wind-sea states within the Gulf of Thailand.[14]

Despite the strategic importance of this region for tourism, fisheries, and offshore petroleum activities, a critical gap remains in the scientific literature. Recent regional studies include a 2023 provincial assessment of central Vietnam[14] and a high-resolution national coastal characterization published in 2026.[12] These studies provide important contemporary benchmarks, but their spatial focus and analysis windows do not resolve the multi-decadal stability, trend behavior, and site-ranking questions addressed here for the southern shelf. Global and regional wave-climate studies further show that wave-power density can be non-stationary and may respond to decadal changes in wind forcing and climate variability.[15,16] For engineering screening and investment planning, understanding how the resource has evolved over multiple decades is therefore as important as estimating its long-term mean.[17-19] Comparable wave-resource assessments for waters bordering China and the Pacific coast of Central America further support the use of spatial, directional, and device-applicability metrics in regional screening frameworks.[20,21]

This study addresses these limitations by presenting a comprehensive regional assessment of wave-energy resources along the southwestern Vietnamese shelf, with a dedicated focus on strategic island locations. Utilizing a high-resolution Delft3D-WAVE/SWAN modeling framework forced by ERA5 wind reanalysis, we provide a continuous 31-year analysis window (1995–2025). The investigation evaluates six representative stations–Phu Quy, Vung Tau, Con Dao, Tra Vinh, Phu Quoc, and Tho Chu–spanning a diverse spectrum of exposure levels and bathymetric settings.

The novelty of this research lies in integrating multi-decadal Mann–Kendall/Sen-slope analysis with a transparent Long-term Suitability Score (LSS) for island-energy screening. Unlike studies focused only on mean energy density, the analysis also quantifies seasonal stability, directional persistence, energetic availability, and extreme-wave exposure through bivariate wave height (Hs)–peak period (Tp) energy matrices. The objectives are to: (i) quantify finite-depth wave-power density across the southern shelf; (ii) identify trends and seasonal shifts over the 31-year period; and (iii) rank candidate locations using normalized, explicitly weighted criteria with a weight-sensitivity check. The resulting LSS is a screening index rather than a device-specific or techno-economic feasibility assessment.

2. Materials and methods

2.1. Study area and data archive

The study area encompasses the southern Vietnamese continental shelf from Vung Tau to Kien Giang, covering approximately 900 km of coastline (Figure 1). Six stations represent offshore-influenced settings (Phu Quy and Vung Tau), the eastern shelf (Con Dao and Tra Vinh), and the sheltered Gulf of Thailand (Phu Quoc and Tho

Chu). Bathymetry was obtained from the 15-arc-second GEBCO grid.[22] Hourly ERA5 10-m zonal and meridional wind components at 0.25° × 0.25° resolution were spatially interpolated to the wave-model grid. The common analysis window extended from January 1, 1995, to December 31, 2025, yielding a 31-year multi-decadal archive.[17,23] The station coordinates, water depths, and environmental classifications are summarized in Table 1.

2.2. Delft3D-WAVE/SWAN model configuration

The wave climate was simulated using the third-generation SWAN model implemented in Delft3D-WAVE.[12,24] The approximately 900 km × 200 km domain used a 428 × 185 orthogonal curvilinear grid, with resolution varying from about 750 m near coastal hotspots to 8,000 m at offshore boundaries. Shorelines were treated as closed energy-absorbing boundaries, while time-varying directional spectra were imposed at open-ocean boundaries. Each simulation segment began from a flat sea and used a 24-h spin-up before hourly output extraction. The spectral action-balance equation is given in **Equation 1**:

Table 1. Locations, water depths, and environmental classification of the six wave-data extraction stations

Station	Lon (deg)	Lat (deg)	Depth (m)	Group
Phu Quy	109.050	10.617	85.6	Island/ offshore
Vung Tau	108.412	9.652	54.7	Offshore
Con Dao	106.881	8.675	25.4	Island/ Offshore
Tra Vinh	107.118	9.498	24.0	Nearshore
Phu Quoc	103.750	10.000	23.8	Island/ Offshore
Tho Chu	103.250	9.250	39.9	Island/ Offshore

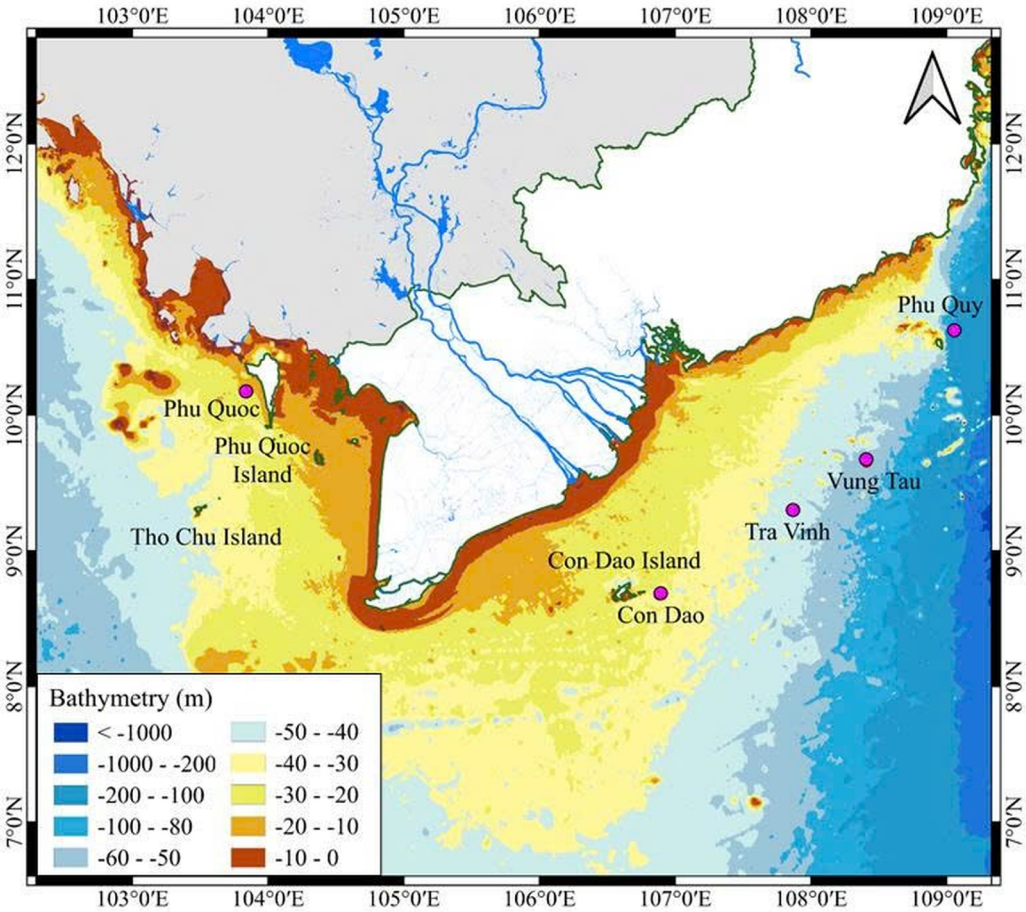

Figure 1. Geographical and bathymetric setting of the southern Vietnamese shelf, showing the Delft3D-WAVE/SWAN domain, bathymetric gradients, major islands, and the six extraction stations used for multi-decadal wave-energy assessment

$$\frac{\partial N}{\partial t}+\frac{\partial c_x N}{\partial x}+\frac{\partial c_y N}{\partial y}+\frac{\partial c_\sigma N}{\partial \sigma}+\frac{\partial c_\theta N}{\partial \theta}=\frac{S_{tot}}{\sigma} \quad (1)$$

where t is time; c_x and c_y are propagation velocities in geographical space; c_σ and c_θ are propagation velocities in spectral space; and S_{tot} is the net source term representing wind input, whitecapping, bottom friction, depth-induced breaking, and nonlinear wave–wave interactions.

2.3. Spectral wave parameters and power estimation

Spectral wave statistics were derived from the directional variance-density spectrum $E(f, \theta)$. The nth spectral moment is defined in **Equation 2**:

$$m_n=\int_0^\infty\int_0^{2\pi} f^n E(f,\theta)\,df\,d\theta \quad (2)$$

Significant Hs and energy period (Te) were estimated as in **Equations 3** and **4**, respectively:

$$H_s=4\sqrt{m_0} \quad (3)$$

$$T_e=\alpha T_{peak} \quad (4)$$

Here, m_0 is the zeroth spectral moment, and α is the period-conversion coefficient, set to 0.90 for this shelf environment following recent regional assessments.[5,14] Wave-power density P per unit crest length (kW/m) under finite-depth conditions was calculated as in **Equation 5**:

$$P=\frac{\rho g H_s^2}{16}C_g\times 10^{-3} \quad (5)$$

Here, ρ = 1,025 kg/m^3 is the seawater density, g = 9.81 m/s^2 is gravitational acceleration, and C_g is the group velocity from linear wave theory (**Equations 6** and **7**):

$$C_g=\frac{1}{2}c\left[1+\frac{2kd}{\sinh(2kd)}\right] \quad (6)$$

$$\omega^2=gk\tanh(kd) \quad (7)$$

In these formulations, c is phase velocity, k is wave number, d is water depth, and ω is intrinsic radian frequency. The dispersion relation in **Equation 7** was solved consistently with the finite water depth at each extraction station.

2.4. Statistical trend and seasonality analysis

Multi-decadal trends were evaluated using the non-parametric Mann–Kendall test and Sen's slope estimator.[15,25] The Mann–Kendall S statistic is shown in **Equation 8**:

$$S=\sum_{i=1}^{n-1}\sum_{j=i+1}^{n}\mathrm{sgn}(x_j-x_i) \quad (8)$$

The variance of S, including the correction for tied values, is shown as in **Equation 9**:

$$\mathrm{Var}(S)=\frac{n(n-1)(2n+5)-\sum_t t(t-1)(2t+5)}{18} \quad (9)$$

The standardized Z statistic identifies trends at the 95% confidence level ($p < 0.05$) (**Equation 10**):

$$Z=\begin{cases}\dfrac{S-1}{\sqrt{\mathrm{Var}(S)}} & S>0\\ 0 & S=0\\ \dfrac{S+1}{\sqrt{\mathrm{Var}(S)}} & S<0\end{cases} \quad (10)$$

Trend magnitude was quantified using Sen's slope β (**Equation 11**):

$$\beta=\mathrm{median}\left[\frac{x_j-x_i}{j-i}\right],\forall j>i \quad (11)$$

Seasonal resource variability was quantified using the Seasonal Variability Index (**Equation 12**):

$$SV=\frac{P_{max,season}-P_{min,season}}{\bar{P}_{annual}} \quad (12)$$

A composite LSS was calculated from six normalized criteria. For a beneficial criterion x, $x' = (x - x_{min})/(x_{max} - x_{min})$; extreme exposure was treated as a cost criterion through $(1-X')$. The base-case score was calculated using **Equation 13**:

$$\mathrm{LSS} = (E' + A' + S' + T' + D' + 1 - X')/6 \quad (13)$$

where E′ is normalized mean energy potential, A′ is energetic availability (P > 2 kW/m), S′ is stability derived inversely from monthly CV, T′ is Sen-slope trend performance, D′ is directional concentration, and X′ is extreme-wave exposure (Hs > 3 m). Equal weights (wi = 1/6; Σwi = 1) were adopted because no expert elicitation or analytic hierarchy process evidence was available to justify preferential weighting. In a one-at-a-time sensitivity test, each weight was varied by ±20%, and all weights were renormalized to sum to one; Phu Quy and Tra Vinh retained ranks 1 and 2 in every case. The LSS is therefore interpreted as a transparent screening index, not a device-specific investment decision.

2.5. Model validation metrics

Model reliability was evaluated using bias, mean absolute error (MAE), root mean square error (RMSE), scatter index (SI), Pearson correlation (R), and Willmott's index of agreement (d).[26] RMSE and d are defined in **Equations 14** and **15**, respectively:

$$\mathrm{RMSE}=\sqrt{\frac{1}{n}\sum_{i=1}^{n}(S_i-O_i)^2} \quad (14)$$

$$d = 1 - \frac{\sum_{i=1}^{n}(S_i - O_i)^2}{\sum_{i=1}^{n}(|S_i - \bar{O}| + |O_i - \bar{O}|)^2} \quad (15)$$

where S_i and O_i are simulated and observed values, respectively, and $\bar{O}$ is the mean of the observations.

3. Results

3.1. Model reliability and statistical validation

The Delft3D-WAVE/SWAN model was evaluated against paired hourly acoustic wave and current observations at Ca Mau (ST1; July 11–18, 2020) and Ben Tre (ST2; July 22–August 1, 2020). Hs skill was strong at ST1 (R = 0.90, d = 0.93, RMSE = 0.09 m) and moderate at ST2 (R = 0.70, d = 0.60, RMSE = 0.28 m). Tp was less accurately reproduced: ST1 yielded R = 0.52 and d = 0.57, while ST2 yielded R = −0.10 and d = 0.25. Accordingly, the model supports regional and multi-decadal Hs-based resource screening, but absolute period-dependent power estimates and device-matching interpretations remain more uncertain. Table 2 reports the complete paired metrics rather than relying only on the best-performing site.

3.2. Spatiotemporal gradient and the sheltering effect

The long-term statistics (1995–2025) reveal a pronounced east-west energy gradient across the southern Vietnamese shelf (Table 3). Phu Quy emerged as the primary energy hotspot with a mean wave-power density of 13.87 kW/m and a 95th-percentile (P_{95}) value of 60.10 kW/m. In stark contrast, Phu Quoc recorded a marginal mean power of only 1.36 kW/m.

This disparity between Phu Quy and Phu Quoc is not merely numerical but physically significant. It confirms the critical role of the Cà Mau peninsula as a geographical barrier that shields the Gulf of Thailand from the high-energy swells of the East Sea. As waves propagate from the open ocean onto the western shelf, island sheltering and energy dissipation over the broad, shallow bathymetry significantly reduce the harvestable resource. This spatial differentiation, visualized in the model domain (Figures 1 and 2), suggests that while the eastern stations offer utility-scale potential, the western stations are better suited for specialized low-energy or hybrid applications.

3.3. Decadal trends and climate signals

Mann–Kendall and Sen-slope estimates identified significant increases in wave power at Phu Quy, Tra Vinh, and Vung Tau (Figure 3; Table 4). Phu Quy had the largest slope (+0.1436 kW/m/yr; p = 0.005), followed by Tra Vinh (+0.0795 kW/m/yr; p < 0.001) and Vung Tau (+0.0563 kW/m/yr; p < 0.001). Con Dao, Phu Quoc, and Tho Chu showed no significant annual-power trends at the 95% confidence level.

These station-specific increases are consistent with a strengthening of the historical northeast-monsoon wave regime on exposed parts of the shelf, but the present wave-only analysis does not isolate a causal atmospheric mechanism. The pattern indicates that resource screening and structural design should account for observed non-stationarity. Direct attribution would require concurrent trend analysis of ERA5 winds and relevant climate indices, while projection beyond 2025 requires scenario-based wave modeling.

3.4. Seasonal contrast and power stability

The regional wave resource varied strongly with season. Eastern-station dominant-direction energy shares ranged from 56.4% to 73.5%, exceeding 70% at Phu Quy and Con Dao (Table 5). Con Dao's mean northeast monsoon power was 6.37 times its southwest monsoon value. Such seasonality reduces the suitability of stand-alone wave generation and motivates evaluation of storage and hybrid generation using coincident resource and load data.

The directional energy roses (Figure 4) and monthly heatmap (Figure 5) reinforce this contrast. The dominant

Table 2. Independent model-validation metrics against paired hourly *in situ* acoustic wave and current observations at Ca Mau and Ben Tre

Validation site, window and paired *n*	Variable (unit)	Bias	Mean absolute error	Root mean square error	Scatter index	*R*	Willmott *d*
Ca Mau	Hs (m)	0.05	0.08	0.09	0.24	0.90	0.93
	Tp (s)	−0.86	0.98	1.13	0.26	0.52	0.57
Ben Tre	Hs (m)	0.16	0.19	0.28	0.84	0.70	0.60
	Tp (s)	−1.23	2.24	3.85	0.81	−0.10	0.25

Abbreviations: Hs: Wave height; Tp: Peak period.

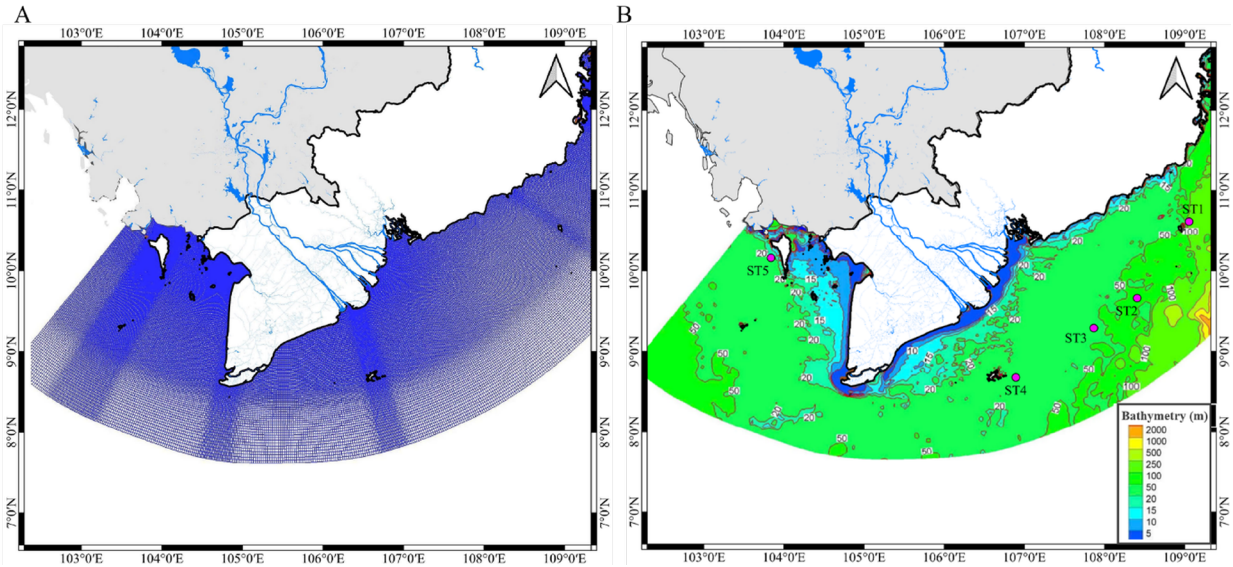

Figure 2. Model domain, nested analysis area, bathymetry, and locations of the six wave-data extraction stations used in the 1995–2025 Delft3D-WAVE/SWAN hindcast and extension analysis. Marker colors indicate station depth, and the dashed box denotes the main analysis domain.

Table 3. Long-term wave-climate and finite-depth wave-power statistics for the six extraction stations

Station	Mean Hs (m)	Mean Tp (s)	Mean energy period (s)	Mean wave-power density (kW/m)	Median wave-power density (kW/m)	P_{95} wave-power density (kW/m)	Hs > 3 m (%)
Phu Quy	1.70	5.57	5.01	13.87	4.85	60.10	12.66
Vung Tau	1.06	4.93	4.43	4.45	1.72	16.32	1.15
Con Dao	1.19	4.94	4.44	6.04	1.94	26.57	3.18
Tra Vinh	1.16	4.83	4.35	5.34	1.89	21.95	1.65
Phu Quoc	0.68	3.76	3.38	1.36	0.50	5.56	0.05
Tho Chu	0.66	3.56	3.21	1.12	0.47	4.42	0.00

Abbreviations: Hs: Wave height; Tp: Peak period.

energy sector contributed 56.4–73.5% at the four eastern stations, with the highest concentration at Phu Quy. This directional consistency can simplify first-stage WEC orientation screening, but the marked transition- and southwest-season reduction means that annual microgrid reliability cannot be inferred from the wave resource alone.

3.5. Bivariate wave height–peak period matrices and wave-energy converter matching

The joint-occurrence and energy-contribution matrices in Figure 6 characterize the sea-state envelopes relevant to preliminary device screening. Phu Quy showed a broad energetic envelope extending to Hs > 3.0 m and Tp = 6–10 s. These descriptors may guide comparison with manufacturer or validated WEC power matrices, but they do not by themselves demonstrate device yield, survivability, or economic feasibility.

Phu Quoc and Tho Chu were concentrated in low-Hs (<1.0 m), short-period (<4 s) conditions and are therefore unlikely to suit conventional devices designed for more energetic seas. Technology matching at these sites would require validated low-threshold power matrices and local survivability constraints. The contrast among the six matrices demonstrates why equal mean power can conceal

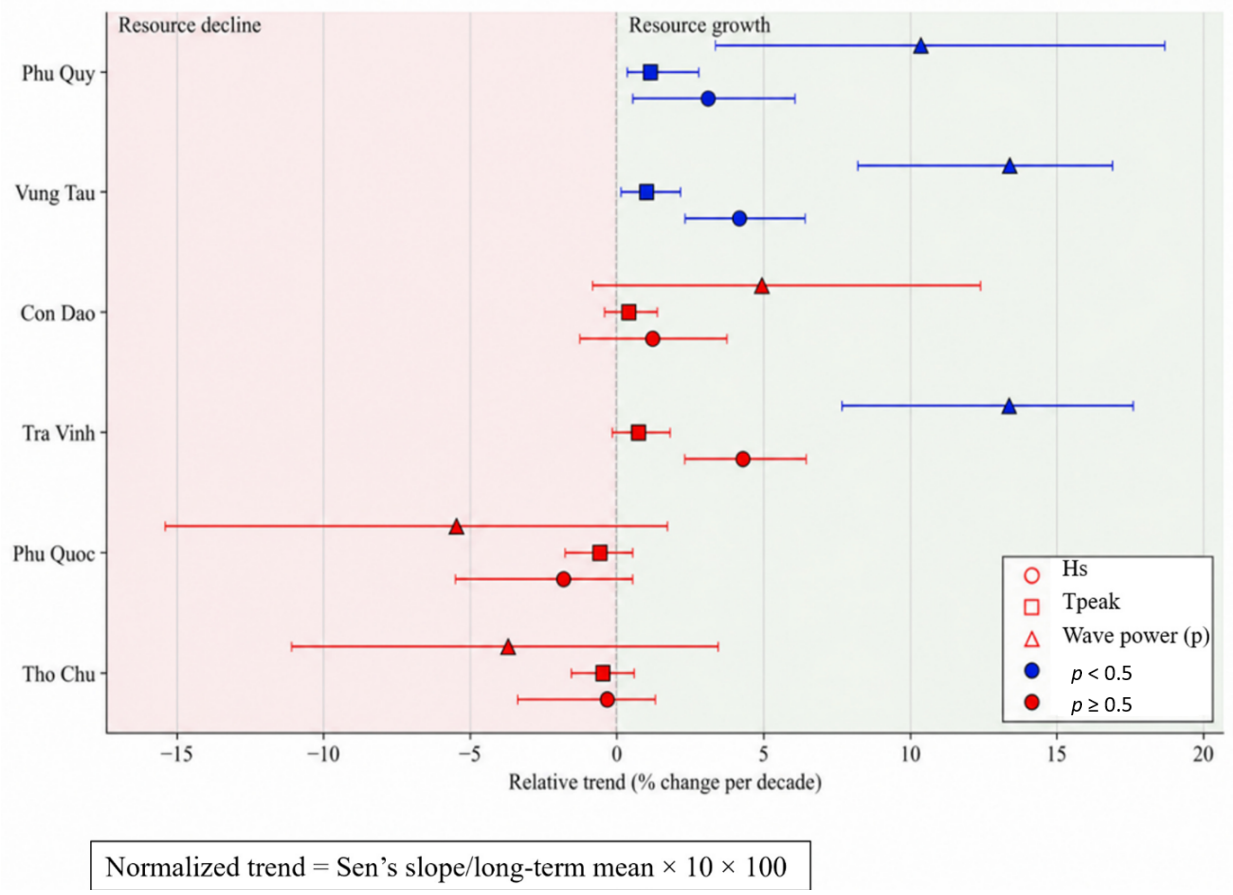

Figure 3. Multi-parameter decadal trend synthesis (1995–2025) for significant wave height (Hs), peak period (Tpeak), and wave power (*P*). Markers represent the relative Sen's slope (% change per decade), with horizontal error bars indicating the 95% confidence interval. Statistical significance ($p < 0.05$ via Mann–Kendall test) is denoted by solid filled markers. The visualization highlights the non-stationary nature of the resource, particularly the quadratic amplification of wave power trends relative to Hs at eastern shelf stations.

Table 4. Mann–Kendall significance and Sen's slope estimates for annual mean Hs, Tp, and wave-power density

Station	Hs slope (m/yr)	Hs *p*	Hs trend	Tp slope (s/yr)	Tp *p*	P slope (kW/m/yr)	P *p*	P trend
Con Dao	0.001	0.39	NS	0.002	0.308	0.029	0.153	NS
Phu Quoc	−0.001	0.11	NS	−0.002	0.359	−0.007	0.153	NS
Phu Quy	0.005	0.01	I	0.006	0.009	0.143	0.005	I
Tra Vinh	0.006	<0.001	I	0.004	0.057	0.079	<0.001	I
Vung Tau	0.006	<0.001	I	0.006	0.013	0.056	<0.001	I
Tho Chu	<0.001	0.84	NS	−0.001	0.324	−0.004	0.292	NS

Note: *p*-values < 0.05 indicate statistically significant trends at the 95% confidence level.
Abbreviations: Hs: Wave height; I: Increasing; NS: Not significant; P: Wave-power density; Tp: Peak period.

Table 5. Seasonal wave-power contrast, seasonal trend signal and directional-energy dominance at the six stations during 1995–2025

Station	NE mean P	SW mean P	Transition mean P	NE/SW ratio	NE β	NE *p*	SW β	SW *p*	Monthly CV	DES	ESS (%)
Con Dao	11.76	1.85	2.46	6.37	0.114	0.012	0.005	0.497	0.97	ENE	70.4
Phu Quoc	0.85	2.11	0.76	0.40	−0.003	0.212	−0.018	0.135	0.61	W	34.8
Phu Quy	26.03	5.01	6.14	5.20	0.316	0.016	0.054	0.089	0.94	NE	73.5
Tra Vinh	10.32	1.52	2.67	6.81	0.175	<0.001	0.018	0.007	0.90	ENE	60.8
Vung Tau	8.22	1.66	2.19	4.95	0.133	<0.001	0.023	0.012	0.83	E	56.4
Tho Chu	0.91	1.53	0.63	0.60	−0.001	0.812	−0.014	0.089	0.50	W	28.4

Abbreviations: CV: Coefficient of variation; DES: Dominant energy sector; E: East; ENE: Eastern northeast; ESS: Energy-sector share; NE: Northeast monsoon; P: Wave-power density; SW: Southwest monsoon; W: West; β: Sen slope.

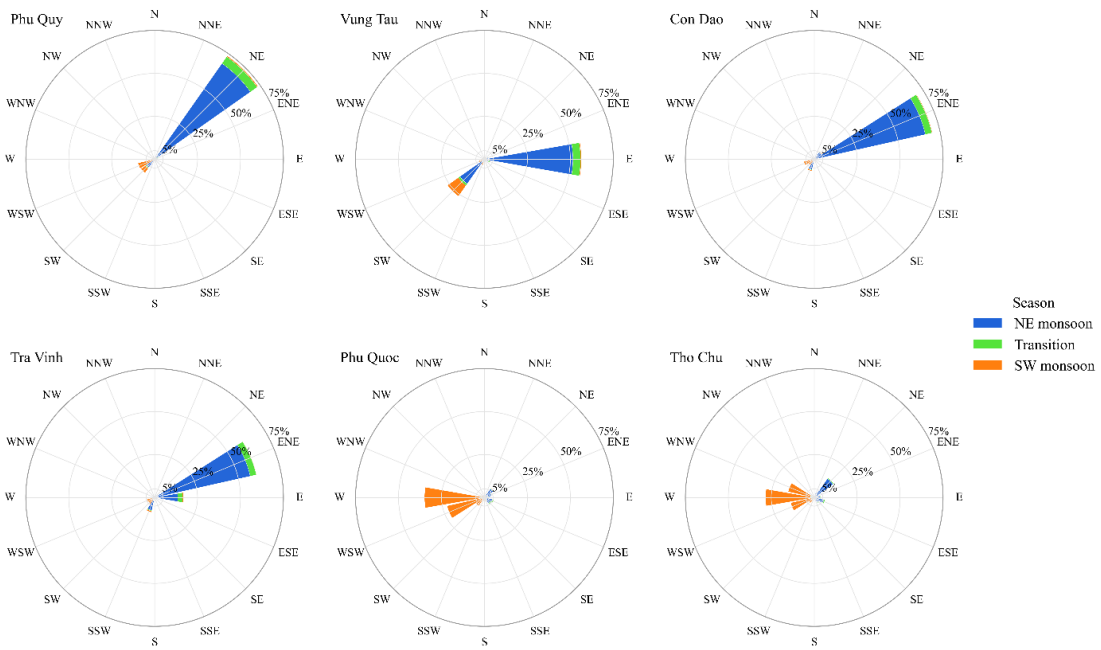

Figure 4. Seasonal energy roses showing the directional contribution to total wave-power density at the six extraction stations during 1995–2025. Bar length indicates each directional sector's energy share, and colors distinguish the northeast (NE) monsoon, transition, and southwest (SW) monsoon seasons.

different operating envelopes; all WEC interpretations here remain screening-level.

4. Discussion

4.1. Comparison with regional and global wave-energy contexts

The annual mean wave-power density of 13.87 kW/m at Phu Quy and 6.04 kW/m at Con Dao places the southern Vietnamese shelf in a "moderate-energy" category compared to other global and regional hotspots. Previous assessments along the central coast of Vietnam[14] reported power levels often exceeding 20–30 kW/m due to direct exposure to deep-water oceanic swells. Globally, oceanic islands in Indonesia and the Philippines can experience

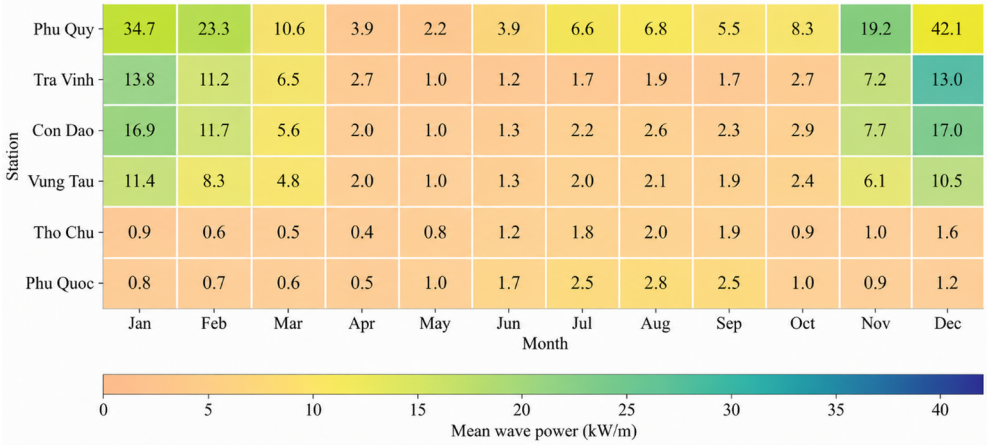

Figure 5. Monthly variability of mean wave-power density at the six extraction stations during 1995–2025. Cell colors and annotated values indicate monthly mean wave power (kW/m), highlighting the strong northeast monsoon energy peak from November to February, especially at Phu Quy, and the comparatively low-energy regimes at Phu Quoc and Tho Chu.

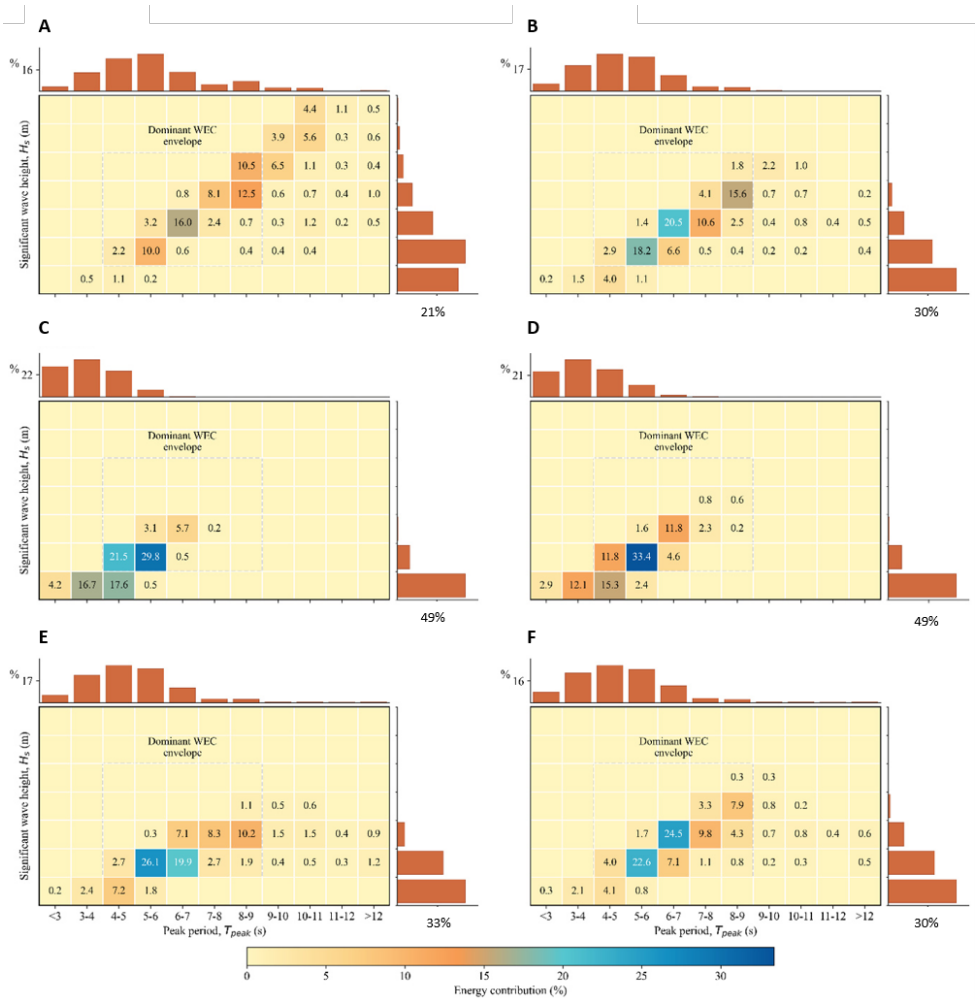

Figure 6. Bivariate wave height (Hs)–peak period (Tp) energy-contribution matrices for all six extraction stations during 1995–2025. Cell colors show each sea-state bin's percentage contribution to total wave-power density; marginal bars show the corresponding Hs and Tp occurrence distributions. The matrices support resource-shape screening and do not represent device power output. (A) Phu Quy. (B) Con Dao. (C) Tho Chu. (D) Phu Quoc. (E) Vung Tau. (F) Tra Vinh.

even higher magnitudes (>40 kW/m) from Pacific swells.

However, the southwestern shelf offers a potentially useful feature: site-specific directional concentration. Across the four eastern stations, the directional concentration index *R* ranged from 0.46 to 0.65 (Table 6), with the highest values at Tra Vinh (0.65), Con Dao (0.61), and Phu Quy (0.59). These moderate concentration levels can inform first-stage WEC orientation and control screening, but they do not by themselves demonstrate simpler yaw control, higher net energy capture, or superior economic performance. Device-specific directional response and power-matrix analyses remain necessary before deployment decisions.

4.2. Climate signals and engineering implications

The significant historical wave-power trends at Phu Quy, Vung Tau, and Tra Vinh are consistent with changes in the northeast-monsoon wave regime reported in recent wind-wave and CMIP6 syntheses.[16,17] However, the present analysis does not regress local wave trends against wind or climate indices; the results therefore demonstrate non-stationary wave conditions rather than formal attribution to monsoon intensification. A recent Pacific Northwest assessment likewise shows that climate scenarios can alter both wave-energy magnitude and variability, reinforcing the need for scenario-based interpretation rather than deterministic extrapolation.[27]

From an engineering perspective, the observed trends justify considering non-stationarity in screening and design-life studies. They should not be extrapolated linearly to claim a specific 2050 increase because no future-climate scenario was simulated. Follow-up work should combine bias-corrected climate projections, extreme-value analysis, fatigue loading, and device-specific survivability models before proposing quantitative future design allowances.

4.3. Resource reliability and proximity to load centers

Choosing the "best" site involves a complex trade-off between energy potential and logistical feasibility. Phu Quy is undoubtedly the leading hotspot in terms of raw power density. However, its distance from the mainland raises the levelized cost of energy because of higher maintenance and subsea cabling costs.

The equal-weight LSS ranks Phu Quy first (0.645) and Tra Vinh second (0.593), followed by Con Dao (0.483) and Vung Tau (0.479). Phu Quy's high energy and trend scores offset its larger extreme-wave exposure, whereas Tra Vinh combines moderate energy, strong directionality, lower extreme exposure, and a positive trend. The two leading ranks remain unchanged under ±20% one-at-a-time weight perturbations. These results support phased site screening, not a final techno-economic deployment decision.

4.4. Practical implications: The hybrid microgrid model

The strong wave-seasonality identified here shows that stand-alone wave generation would require substantial balancing. A wave–solar–wind–storage microgrid

Table 6. Equal-weight Long-term Suitability Score and site-screening rank

Station	Mean P (kW/m)	P > 2 kW/m (%)	P slope (kW/m/yr)	Directional *R*	Hs > 3 m (%)	LSS	Rank	Screening interpretation
Phu Quy	13.87	67.6	0.144	0.59	12.66	0.645	1	Leading offshore site
Tra Vinh	5.34	48.8	0.079	0.65	1.65	0.593	2	Leading nearshore site
Con Dao	6.04	49.2	0.030	0.61	3.18	0.483	3	Device-specific screening
Vung Tau	4.45	46.6	0.056	0.46	1.15	0.479	4	Device-specific screening
Phu Quoc	1.36	17.5	−0.007	0.43	0.05	0.353	5	Sheltered hybrid option
Tho Chu	1.12	15.2	−0.004	0.34	0.00	0.337	6	Sheltered hybrid option

Note: All criteria were min–max normalized. Each base weight equals 1/6, and the weights sum to one. The first two ranks remain unchanged when each criterion weight varies by ±20%, and the weights are renormalized. LSS is a screening index, not a device-specific techno-economic decision.
Abbreviations: Hs: Wave height; LSS: Long-term Suitability Score; P: Wave-power density.

is a plausible diversification option, but its seasonal complementarity must be tested, not assumed.

Wave power is strongest during the northeast-monsoon months and weakens during much of the southwest monsoon. In southern Vietnam, the southwest monsoon broadly overlaps the wetter and cloudier season, so solar output cannot be assumed to reach its annual maximum when wave power is lowest. A defensible hybrid design requires coincident hourly wave, irradiance, wind, storage, and electrical-load series, followed by reliability and cost optimization. The present results identify the wave component and its seasonal deficit but do not quantify hybrid-system performance.

5. Conclusion

This study provides a 31-year assessment (1995–2025) of wave-energy resources across the southern Vietnamese shelf. The analysis identifies a strong east–west gradient, marked monsoon seasonality, and station-specific historical trends. Model validation supports regional Hs-based screening, while weaker Tp performance at Ben Tre requires caution when interpreting period-dependent power and device performance.

Phu Quy is the primary resource hotspot (mean P = 13.8 kW/m; P_{95} = 60.1 kW/m). Significant power increases occurred at Phu Quy (+0.143 kW/m/yr), Tra Vinh (+0.079 kW/m/yr), and Vung Tau (+0.056 kW/m/yr). Dominant-direction shares across the eastern stations ranged from 56.4% to 73.5%, showing both directional persistence and strong seasonal concentration. The transparent equal-weight LSS ranked Phu Quy and Tra Vinh first and second, and these ranks were stable to ±20% criterion-weight perturbations.

The results provide a reproducible screening basis for marine spatial planning and phased pilot studies. They do not establish device-specific yield, economic feasibility, future climate change, or seasonal wave–solar complementarity. Those parameters require validated WEC power matrices, high-resolution scenario modeling, extreme and fatigue analysis, and coincident hybrid-resource and demand data.

Acknowledgments

None.

Funding

This research was funded by Vietnam National University Ho Chi Minh City (VNU-HCM) under a project (grant number CB2025-20-27) within the framework of the Program titled "Strengthening the capacity for education and basic scientific research integrated with strategic technologies at VNU-HCM," aiming to achieve advanced standards comparable to regional and global levels during the 2025–2030 period, with a vision toward 2045.

Conflict of interest

The authors declare they have no competing interests.

Author contributions

Conceptualization: Tran Thi Mai Huong, Le Thanh Phong, Nguyen Tuan, Nguyen Xuan Kha
Formal analysis: Tran Thi Mai Huong, Dang Truong An
Methodology: Tran Thi Mai Huong, Dang Truong An
Writing–original draft: Tran Thi Mai Huong, Dang Truong An
Writing–review & editing: Tran Thi Mai Huong, Dang Truong An

Availability of data

Data used in this study are available from the corresponding author upon reasonable request.

References

1. Wilk-Jakubowski JL, Pawlik L, Wilk-Jakubowski G, Harabin R. State-of-the-Art in the Use of Renewable Energy Sources on the Example of Wind, Wave Energy, Tidal Energy, and Energy Harvesting: A Review from 2015 to 2024. *Energies*. 2025;18(6):1356.

   doi: 10.3390/en18061356

2. Tang E, Gao J, Huang W, Qian Y. Marine renewable energy: Progress, challenges, and pathways to scalable sustainability. *Energy*. 2025;335:138083.

   doi: 10.1016/j.energy.2025.138083

3. Wu JJ, Vijayamohan V, Field RW. On the potential of ocean energy technologies to contribute to future sustainability. *Discov Sustain*. 2025;6(1):132.

   doi: 10.1007/s43621-025-01676-x

4. Bouhrim H, El Marjani A, Nechad R, Hajjout I. Ocean Wave Energy Conversion: A Review. *J Mar Sci Eng*. 2024;12(11):1922.

   doi: 10.3390/jmse12111922

5. Li H, Shi X, Kong W, *et al*. Advanced wave energy conversion technologies for sustainable and smart sea: A comprehensive review. *Renew Energy*. 2025;238:121980.

   doi: 10.1016/j.renene.2024.121980

6. Zhou B, Zheng Z, Yao Y, *et al*. Wave energy converters: a comprehensive review of research progress, key challenges, and future trends. *Appl Energy*. 2026;413:127722.

   doi: 10.1016/j.apenergy.2026.127722

7. Arrosyid WA, Sari WR, Waskito KT, *et al*. Recent advancements in wave energy converter technologies: A comprehensive review on design and performance optimization. *Ocean Eng*. 2025;340:122328.

doi: 10.1016/j.oceaneng.2025.122328

8. Song H, Yu T, Tong X, *et al*. Hybrid Offshore Wind and Wave Energy Systems: A Review. *Energies*. 2026;19(3):739.

doi: 10.3390/en19030739

9. Kaur N, Sudhakar K, Mohamed MR, B R, Barbulescu D. Offshore hybrid renewable energy: insights from real-world implementations. *Front Energy Res*. 2026;14:1779158.

doi: 10.3389/fenrg.2026.1779158

10. Konispoliatis DN. Floating Oscillating Water Column Wave Energy Converters: A Review of Developments. *J Energy Power Technol*. 2024;6(1):1-29.

doi: 10.21926/jept.2401005

11. Marques Silva J, Vieira SM, Valério D, Henriques JCC. Model predictive control based on air pressure forecasting of OWC wave power plants. *Energy*. 2023;284:129217.

doi: 10.1016/j.energy.2023.129217

12. Nguyen TTD, Wang XH. Wave-Resource Characterization Along the Coast of Vietnam. *Geosciences*. 2026;16(5):189.

doi: 10.3390/geosciences16050189

13. Hu X, Fang Y, Wu Y, Wu H, Kang HS. An approach to assess the potential of wave energy resources based on directional energy flux. *Ocean Eng*. 2023;287:115732.

doi: 10.1016/j.oceaneng.2023.115732

14. Tung TT, Chien NQ. Assessment of potential wave power along a coastal province, Central Vietnam. *Int J Mar Energy*. 2023;6(1):27-35.

doi: 10.36688/imej.6.27-35

15. Ahn S, Neary VS. Investigation of mixed long-term nonstationary trends in global wave energy systems. *J Clean Prod*. 2024;476:143758.

doi: 10.1016/j.jclepro.2024.143758

16. Casas-Prat M, Hemer MA, Dodet G, *et al*. Wind-wave climate changes and their impacts. *Nat Rev Earth Environ*. 2024;5(1):23-42.

doi: 10.1038/s43017-023-00502-0

17. Xu J, Li J, Pan S, Yao Y, Chen L, Wu Z. Assessment of wind and wave energy in China seas under climate change based on CMIP6 climate model. *Energy*. 2024;310:133207.

doi: 10.1016/j.energy.2024.133207

18. Zhu X, Huang W. Assessing extreme significant wave height in China's coastal waters under climate change. *Front Mar Sci*. 2024;11:1494127.

doi: 10.3389/fmars.2024.1494127

19. Mahmoodi K, Fard HR, Böling J. Long-term climate change effects on power performance of wave energy converters: A case study. *Energy*. 2025;326:136101.

doi: 10.1016/j.energy.2025.136101

20. Wu Y, Zhou Q, Jiang W, Bai Y, Wu H. Wave characteristics and wave energy resource assessment of the waters bordering China. *Front Mar Sci*. 2026;13:1777065.

doi: 10.3389/fmars.2026.1777065

21. Corrales-Gonzalez M, Lavidas G, Lira-Loarca A, Besio G. Wave energy assessment and wave converter applicability at the Pacific coast of Central America. *Front Energy Res*. 2024;12:1454275.

doi: 10.3389/fenrg.2024.1454275

22. GEBCO Bathymetric Compilation Group 2023. The GEBCO_2023 Grid - a continuous terrain model of the global oceans and land. Published online 2023.

doi: 10.5285/F98B053B-0CBC-6C23-E053-6C86ABC0AF7B

23. Al-Badi A, AlHinai J, Al Wahaibi A, Al-Yahyai S. Wave Energy Potential Assessment Along the Coast of Oman. *Energies*. 2026;19(10):2356.

doi: 10.3390/en19102356

24. deCastro M, Rusu L, Arguilé-Pérez B, *et al*. Different approaches to analyze the impact of future climate change on the exploitation of wave energy. *Renew Energy*. 2024;220:119569.

doi: 10.1016/j.renene.2023.119569

25. Arguilé-Pérez B, Costoya X, Ribeiro AS, deCastro M, Carracedo P, Gómez-Gesteira M. High-Resolution Wave Climate Data under Future Climate Scenarios along the European Atlantic Coast. *Sci Data*. 2026;13(1):412.

doi: 10.1038/s41597-026-07158-7

26. Willmott CJ. On the validation of models. *Phys Geogr*. 1981;2(2):184-194.

doi: 10.1080/02723646.1981.10642213

27. Baghaei M, Rabczuk T, Anitescu C, Bamdad M, Goharnejad H. Wave energy assessment in the Pacific Northwest under historical and future climate conditions: a case study of the Canadian and U.S. coasts. *J Ocean Eng Mar Energy*. 2026;12(3):1557-1582.

doi: 10.1007/s40722-026-00502-4